Standoff Detection of High Explosive Materials at 50 Meters in Ambient Light Conditions Using a Small Raman Instrument

J. CHANCE CARTER,* S. MICHAEL ANGEL, MARION LAWRENCE-SNYDER, JON SCAFFIDI, RICHARD E. WHIPPLE, and JOHN G. REYNOLDS

Lawrence Livermore National Laboratory, M division/Forensic Science Center, 7000 East Ave, L-178, Livermore, California 94550 (J.C.C.); Lawrence Livermore National Laboratory, Forensic Science Center, 7000 East Ave, L-178, Livermore, California 94550 (R.E.W., J.G.R.); and University of South Carolina, Dept. of Chemistry and Biochemistry, 631 Sumter Str., Columbia, South Carolina 29208 (S.M.A., M.L.-S., J.S.)

We have designed and demonstrated a standoff Raman system for detecting high explosive materials at distances up to 50 meters in ambient light conditions. In the system, light is collected using an 8-in. Schmidt–Cassegrain telescope fiber-coupled to an *f*/1.8 spectrograph with a gated intensified charge-coupled device (ICCD) detector. A frequency-doubled Nd : YAG (532 nm) pulsed (10 Hz) laser is used as the excitation source for measuring remote spectra of samples containing up to 8% explosive materials. The explosives RDX, TNT, and PETN as well as nitrate- and chlorate-containing materials were used to evaluate the performance of the system with samples placed at distances of 27 and 50 meters. Laser power studies were performed to determine the effects of laser heating and photodegradation on the samples. Raman signal levels were found to increase linearly with increasing laser energy up to ~3×10^6 W/cm^2 for all samples except TNT, which showed some evidence of photo- or thermal degradation at higher laser power densities. Detector gate width studies showed that Raman spectra could be acquired in high levels of ambient light using a 10 microsecond gate width.

Index Headings: **Standoff Raman; Energetic materials; TNT; RDX; PETN.**

INTRODUCTION

High explosive (HE) detection is becoming more important, with suicide bomber and vehicle-borne improvised explosives device (VBIED) activity increasing as of late. With the availability of conventional military explosives due to regime changes and the proliferation of information on the internet regarding methods of producing improvised explosive devices (IED), more comprehensive and sensitive methods of HE detection are needed.

Current HE detection methods span the range from simple colorimetric screening[1–8] to more sophisticated speciation with advanced spectroscopic measurements.[9–16] These techniques generally require contact or proximal sampling, which can be extremely hazardous or ineffective if the device detonates. This makes obvious the need for reliable, remote, or standoff detection methods to reduce the danger of exposure of first responders, law enforcement, and military, to provide early warning to prevent civilian casualties, and to provide tracking for potential attribution. The National Research Council Report on Existing and Potential Standoff Explosives Detection Techniques[17] delineates several optical techniques that have the potential for meeting the needed standoff requirements. Of these, the only Raman technique considered is the specialized, nonlinear technique known as coherent anti-Stokes Raman (CARS),[18] which is more complex than the linear Raman technique (i.e., spontaneous Raman) described in this paper.

Raman spectroscopy has been shown to be an effective technique for analyzing highly energetic materials. Raman is a powerful technique for molecular analysis, suitable for detecting both organic and inorganic materials in any state (solid, liquid, gas). Raman provides direct information about the molecular structure and composition of a sample. The vibrational spectrum provided by Raman is a molecular ''fingerprint'' that can be used to differentiate the sample from a complex media or differentiate very similarly structured molecules from one another and often provides unambiguous sample identification. Numerous reports[19–28] have demonstrated the capabilities of Raman spectroscopy for identifying the classes of nitro-containing and non-nitro-containing explosives using systems that require close proximity with the HE sample. In fact, some government agencies, forensic laboratories, and law enforcement agencies employ benchtop Raman spectroscopic systems for this purpose.

An area of Raman that is seeing renewed interest is standoff Raman spectroscopy, driven largely by NASA's planetary exploration program.[29–33] In standoff Raman, a pulsed laser is used to interrogate a sample from a distance (e.g., tens of meters to kilometers) from which the inelastically Raman scattered photons are collected with a large optic and detected with a dispersive spectrograph system. Such standoff systems were first proposed in the 1970s by T. Hirschfeld.[34] Raman Lidars based on large mounted telescopes and high-powered lasers have been used for two decades for atmospheric measurements at kilometer distances.[35,36] Raman measurements of solids, liquids, and gases have been demonstrated at distances up to several hundred meters using a medium-powered UV laser and a large collection optic.[37,38] However, the first demonstration of a portable standoff Raman system at tens of meters was reported by Angel[39] for organic analysis in large underground storage tanks. Soon thereafter, small telescope-based standoff Raman systems with continuous wave (CW) diode lasers were demonstrated for measuring minerals and other inorganic species. In

Received 18 February 2005; accepted 17 March 2005.

* Author to whom correspondence should be sent. E-mail: carter45@llnl.gov.

0003-7028/05/5906-0769$2.00/0

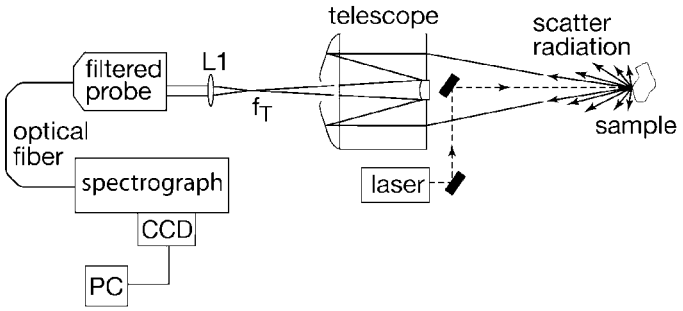

FIG. 1. Schematic diagram of a fiber-coupled, standoff, pulsed Raman spectrograph-based system with gated ICCD detection.

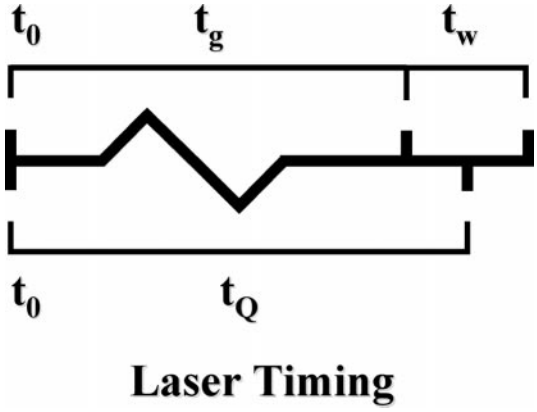

FIG. 2. Synchronization between the laser and detector was controlled by externally triggering both the laser and detector, keeping the laser Q-switch delay constant (t_Q) and adjusting the ICCD gate delay (t_g) to center the ICCD exposure time (t_w) on the frequency-doubled Nd:YAG laser pulse.

recent years, portable standoff systems have been demonstrated for analysis of minerals and inorganic materials using pulsed lasers coupled to small telescopes and highly efficient spectrometers.[31,32,40] In this paper we present Raman measurements of high explosive materials and simulants using such a system at distances up to 50 meters.

EXPERIMENTAL

Equipment. The experimental setup for the prototype standoff pulsed Raman spectrograph based system is schematically shown in Fig. 1. The prototype system consists of a spectrograph equipped with an intensified charge-coupled device (ICCD) detector, a telescope, a holographic filtered-fiber probe, and a frequency-doubled Nd:YAG laser (532 nm, 10 Hz). The maximum power of the laser at 532 nm is ~140 mJ per pulse, the width of the laser pulse is approximately 5 nanoseconds (ns), and the beam divergence is ~1 mrad. The laser is mounted beside the telescope and two 532 nm mirrors are used to bring the beam to the center of the telescope to make it coaxial to the telescope field of view (Fig. 1). Coaxial illumination maximizes the collection efficiency of Raman scattered photons and allows Raman measurements at different distances without system realignment.

The telescope (Celestron, Schmidt–Cassegrain, 200 mm clear aperture, 2000 mm focal length, $f/10$) is coupled to the spectrograph with an optical fiber (non-imaging, 100 micrometer-diameter) probe[41] (Kaiser Optical Systems, Inc., Model Mark II) containing the appropriate filters for rejection of silica Raman scattering and laser radiation. A lens (L1) collimates the light from the telescope output, which is directed into the filtered probe from which the focusing objective has been removed. The output of the fiber is directly coupled to the spectrograph, which contains a pre-filter section with an additional holographic laser rejection filter and fiber coupling optics.

The spectrograph (Kaiser Optical Systems, Model Holospec $f/1.8$) has an entrance aperture ratio of $f/1.8$ and produces an image magnification of unity at the exit plane. The optical axis has a unique on-axis configuration that utilizes a volume phase (VP) holographic diffraction transmission grating for imaging. This design provides spectral dispersion with a high diffraction efficiency (60%) and resulting spectral resolution (11 cm^{-1}) and throughput relative to standard gratings.

Raman spectra were recorded using a thermoelectrically cooled, gated, ICCD (I-MAX-1024-E, 18/G/II P43). The ICCD array is 1024 × 256 pixels and each pixel dimension is 26 × 26 μm^2. A 1 μs gate width was used for all experiments with the exception of the gate width studies, which covered the range from 200 ns to 100 ms. For the spectrograph setup shown in Fig. 1, the detector was mounted such that the Raman spectra were dispersed in the horizontal dimension along the 1024 pixel direction of the CCD. The signal in the vertical dimension (256 pixel) was binned to produce a single-channel signal from each of the 1024 columns of pixels. The horizontal pixels were binned by groups of 2 or 4, depending upon the experiment, to improve signal-to-noise ratio (SNR). A plot of vertical binned signal versus horizontal channels formed the Raman spectra. It is important to note that the spectrograph setup allows an entire Raman spectrum to be acquired with each laser shot.

Laser/Detector Timing. Synchronization between the frequency-doubled Nd:YAG laser (Surelite III, Continuum/Quantronix) and ICCD was controlled with a commercially available timing generator (DG535, Stanford Research Systems, Sunnyvale, CA), with the general timing scheme shown in Fig. 2. Laser flashlamp firing at t_0 was followed by an ICCD gate delay (t_g, typically 224.9 μs), chosen to temporally center the detector exposure time/gate width (t_w, typically 1 μs) on the 5 nanosecond, 532 nanometer laser pulse emitted upon Q-switch triggering at t = 225.4 μs. In cases where longer exposure times were used to study the effect of gate width on the Raman spectra, the gate delay was adjusted to ensure that the exposure time remained centered on the laser pulse (e.g., t_g = 220.4 μs for t_w = 10 μs, t_g = 175.4 μs for t_w = 100 μs, etc.) It is important to note that range-resolved measurements were not part of this study, although these measurements can be performed by varying the delay between the laser pulse and the opening of the ICCD electronic shutter.

Procedures. For evaluating the performance of the standoff pulsed Raman system, high explosive samples of TNT (2,4,6-trinitrotoluene; 2-methyl-1,3,5-trinitrobenzene), RDX (cyclonite; hexagen; hexahydro-1,3,5-trinitro-1,3,5-triazine), PETN (pentaerythritol tetranitrate; 2,2-bis[(nitroxy)methyl]-1,3-propanediol, dinitrate), ni-

trate and chlorate simulants in a dry silica matrix (i.e., sand) were purchased from the XM division of Van Aken International. Each silica-based sample contained approximately 8% HE material except the PETN silica-based sample, which was 4%. These silica-based materials are routinely used by law enforcement and the FAA as canine training aids for HE detection. All samples were used without further preparation by pouring into small nonfluorescent laboratory vials and placing a small piece of aluminum foil inside the vial but behind the samples to minimize fluorescence from the plastic cap. The vials were turned end-on and aligned with the pulsed laser spot. At a distance of 27 meters, the laser pulse spot size matched the diameter (~7 cm) of the sample vial. The telescope field of view (FOV) was slightly larger than the diameter of the laser spot and vial, thereby maximizing the excitation and collection efficiency. The 27 m length distance was chosen because it was the longest hallway available for these experiments. To achieve Raman measurements over a greater distance (i.e., 50 meters), a flat square mirror measuring 2 × 2 inches was placed ~27 m from the telescope and used to reflect both the laser spot and Raman signal. The mirror was mounted at a very slight downward angle toward the floor so that the HE samples could be placed below the telescope collector approximately 1 ft above the floor.

Data Handling. Two commercially available software programs were used for data collection and analysis with the standoff Raman system. Princeton Instruments Winspec 32-bit Windows® software package from Roper Scientific was used for spectral data acquisition. Further processing of the spectral data was carried out using IGOR pro software from Wavemetrics, Inc.

System Detection Efficiency Estimation. The detection efficiency of the system can be estimated from the product of the laser spot size/telescope FOV function, the collection solid angle (sr), transmission of the collection and measurement system (unitless), and the detector quantum efficiency (unitless). The diameter of the laser spot size at the sample for the 27 m measurements was ~7 cm, making the area viewed ~38 cm^2. The telescope field of view (FOV) at the same distance was slightly larger than this, ensuring that the laser spot was completely within the telescope FOV. The solid angle is calculated to be 4.4×10^{-5} sr (8 in. diameter telescope). Because Raman photons scatter in all directions, the solid angle (sr) must be divided by 4π. The collection optics and spectrometer transmission are estimated to be 0.25 (unitless). The ICCD quantum efficiency is 0.08 at 558 nm (i.e., 880 cm^{-1} RDX Raman band). Therefore, the estimated system detection efficiency is $\sim 7 \times 10^{-8}$.

RESULTS AND DISCUSSION

Standoff Detection and Signal-to-Noise Ratio Comparisons of RDX at a Distance of 27 Meters. The Raman spectra of RDX acquired at a distance of 27 meters in ambient light conditions using 1000 (S/N = ~1000) and 10 (S/N = ~100) laser shots are shown in Figs. 3a and 3b, respectively. The S/N calculations were based on the baseline subtracted peak intensity of the most intense peak in the RDX spectrum divided by the root-mean-square (rms) noise. The rms noise was estimated by taking one-fifth the peak-to-peak variation for the flattest region of the Raman spectra between 1850 and 2000 cm^{-1} (region not shown). The Raman spectrum acquired with 10 laser shots (i.e., 1 s integration) is sufficient to identify the sample as RDX. These spectra were used to make a crude estimate of the maximum detectable range for RDX, assuming all factors remain the same such as sample concentration and power density at the sample. Based on the $1/r^2$ (i.e., distance) dependence of signal intensity we can estimate that the Raman signal for an RDX sample at 270 m from the telescope would be similar to that shown in Fig. 3b. Obviously such a calculation does not take into account certain background issues such as ambient light and detector noise. But, it does give some idea of the potential of the technique. The Fig. 3a Raman spectrum of RDX (8% sample composition) was also used to estimate the detection limit (i.e., three times the standard deviation, STD, of the background). By determining the STD (one-fifth peak-to-peak variation) of the background for Fig. 3a and applying a scaling factor to reduce the background-subtracted Raman signal to three times the calculated background STD, we estimate that the detection limit of RDX is approximately 250 parts-per-million (i.e., 0.08/325) for 1000 laser shots. This estimate includes no resonance enhancement effects. It is important to note that the 27-meter Raman data provided the best overlap between the collection optic and laser spot size, allowing for very efficient collection and the best estimation of the S/N for any of the distances studied. Given the available laboratory space, 27 m was the maximum distance available for direct line-of-sight measurements. For comparison with RDX, Fig. 4 shows the Raman spectra of other HE materials acquired using 1000 laser shots at a distance of 27 meters.

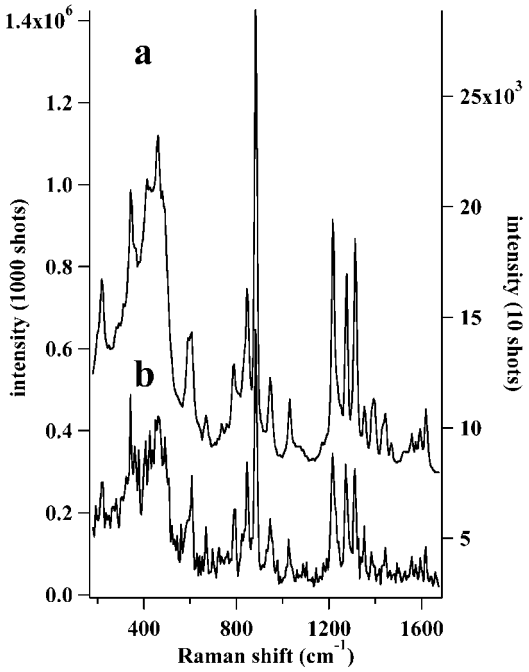

FIG. 3. S/N comparison of Raman spectra of RDX in a silica matrix acquired with (***a***) 1000 laser shots (100 s integration) and (***b***) 10 (1 s integration) laser shots, respectively, in ambient light conditions at a distance of 27 meters using the standoff, pulsed Raman system with gated ICCD detection.

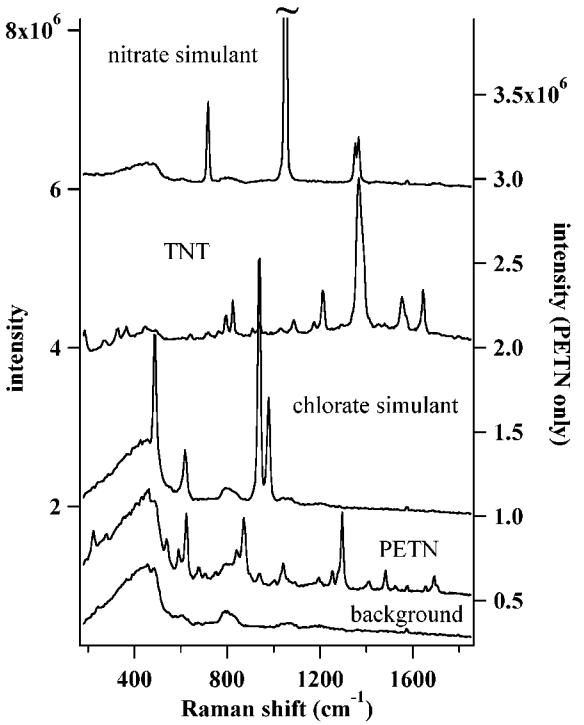

FIG. 4. Raman spectra of TNT, PETN, and nitrate and chlorate simulants in a silica matrix acquired in ambient light conditions at a distance of 27 meters using a standoff, pulsed Raman system with gated ICCD detection.

Standoff Detection of HE Materials at a Distance of 50 Meters. Due to laboratory space limitations, a mirror was used to double the distance over which measurements could be made. To achieve this, a 2 × 2 inch flat mirror was placed ~27 meters from the telescope and used to reflect the laser onto the sample and collect Raman scattered photons for a total distance of 50 m. Unfortunately, this was the largest flat mirror available and the poor overlap between the area of the flat mirror and the image of the telescope at this distance resulted in ~70% signal losses, or approximately one-third the signal that would be expected from using a 4 in. diameter flat mirror. Figures 5a and 5b show Raman spectra, as labeled, of TNT, RDX, PETN, nitrate and chlorate simulants, and silica background acquired in ambient light conditions at a distance of 50 meters using 10 000 laser shots, except for PETN, which required 20 000 shots. The apparent peak located just below 1600 cm^{-1} in all Fig. 5a (and Fig. 4) spectra, including the background spectrum, is a damaged area of the ICCD detector. PETN is shown separately in Fig. 5b and the artifact peak has also been removed in the figure. The spectral features shown for the silica matrix sample in Fig. 5b are due to silica background from the glass vial sample holder as well as the silica matrix.

Laser Power Study of HE Samples at 27 Meters. The high peak power for the pulsed laser can create photo- and thermal induced damage at certain power thresholds, and this threshold is sample dependent.[42–45] Thus, the effect of laser power on the intensity of Raman for each HE sample was determined. Figure 6 shows a plot of Raman peak intensity versus laser power density for RDX and TNT. For all HE samples/simulants, except

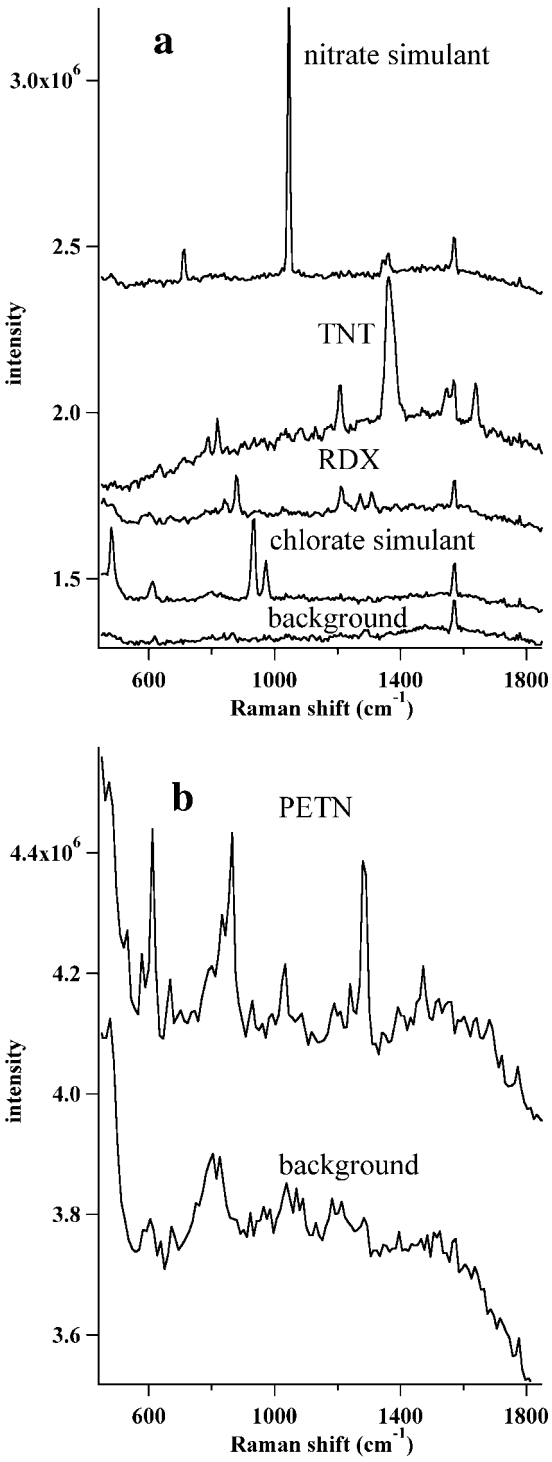

FIG. 5. Raman spectra of (**a**) TNT, RDX, and nitrate and chlorate simulants and (**b**) PETN in a silica matrix acquired in ambient light conditions with 10 000–20 000 laser shots at a distance of 50 meters using a standoff, pulsed Raman system with gated ICCD detection. A small flat mirror was used to double the distance over which measurements could be made due to laboratory space limitations. This resulted in ~70% signal losses due to poor excitation and collection overlap.

TNT, the Raman intensity is roughly linear up to ~3 × 10^6 W/cm^2, after which the Raman signal begins to level off, even though no obvious photo- or thermal degradation was observed upon visual inspection. The linearity shown for the RDX sample is representative of similar

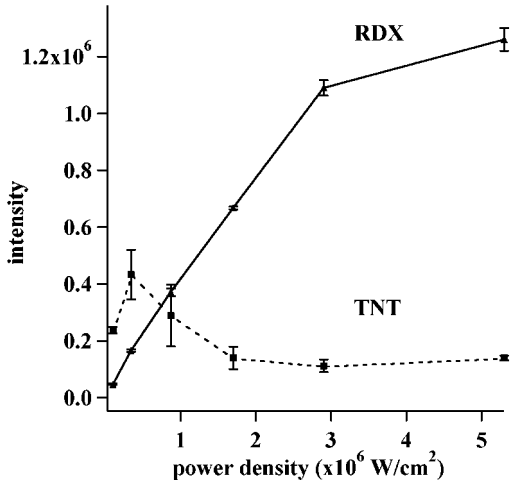

FIG. 6. Laser power studies showing the effects of laser heating and photodegradation on samples of TNT and RDX using the most intense Raman peaks. Raman signal levels were found to increase linearly with increasing laser energy up to $\sim 3 \times 10^6$ W/cm^2 for all samples except TNT, which showed some evidence of photo- or thermal degradation at higher laser power densities.

plots (not shown) for PETN, chlorate simulant, and nitrate simulant. As shown, TNT degrades at a much lower power. Also, there was direct visual evidence of TNT photo- or thermal degradation by virtue of darkened areas on the TNT containing silica matrix surface when exposed to pulse energies as low as $\sim 3.4 \times 10^5$ W/cm^2. This is indicated in Fig. 6 as the Raman intensity quickly levels out beginning around 1.7×10^6 W/cm^2. This demonstrates the importance of optimizing the laser power conditions for the most photolabile HE materials that could potentially be present in an unknown sample. Thermal or photodegradation of an HE component due to high laser energy could potentially lead to false negative results.

Gate Width Studies. The principal advantage of pulsed laser excitation coupled with gated ICCD detection is the ability to record Raman spectra in ambient light conditions and to perform range-resolved measurements (no range-resolved experiments were performed as part of this study). Previous authors have reported stand-off pulsed Raman experiments typically using ≤ 1 μs gate widths with dispersive-based systems in laboratory ambient light conditions.[31,46] However, no published reports have systematically evaluated the effects of gate width for acquiring Raman data in ambient light conditions with a dispersive-based system. For these studies, Raman spectra were recorded for RDX at 27 m with all the fluorescent ceiling lights turned on. Measurements were made with the laser on and off so that the ambient and Raman signals could be independently determined. Figures 7a and 7b show Raman spectra with room lights on for two representative gate widths, 99 ms and 100 μs, respectively. The spectrum acquired with a gate width of 99 ms is dominated by mercury peaks (Hg lines) from room lights, especially the strong 546 nm Hg line. All spectra acquired with gate widths longer than about 10 ms were similar in this regard and had higher ambient background signals. Although, for the HE samples in this study, the strong 546 nm line does not prevent unambiguous identification of the samples, in general high ambient background signals seriously degrade the quality and S/N of the Raman spectra. As shown in Fig. 7b, reducing the detector gate width greatly reduces the ambient light signal without affecting the Raman signal.

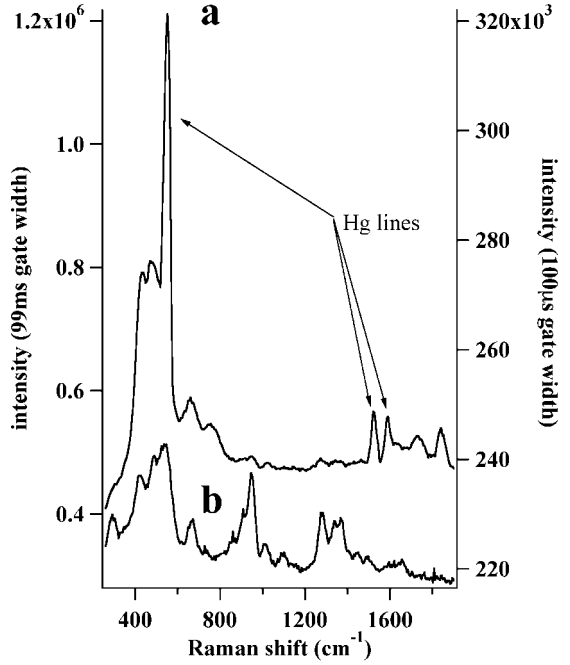

FIG. 7. Detector gate width studies showing the resulting Raman spectra of RDX (880 cm^{-1} peak) acquired in ambient light conditions at a distance of 27 m with (***a***) 99 ms and (***b***) 100 μs gate widths. The 99 ms Raman spectra is dominated by intense Hg lines from fluorescent ceiling lights.

The effect of detector gate width on the Raman and ambient light signals is shown in Fig. 8. In Fig. 8 the most intense peak (background subtracted) in the RDX

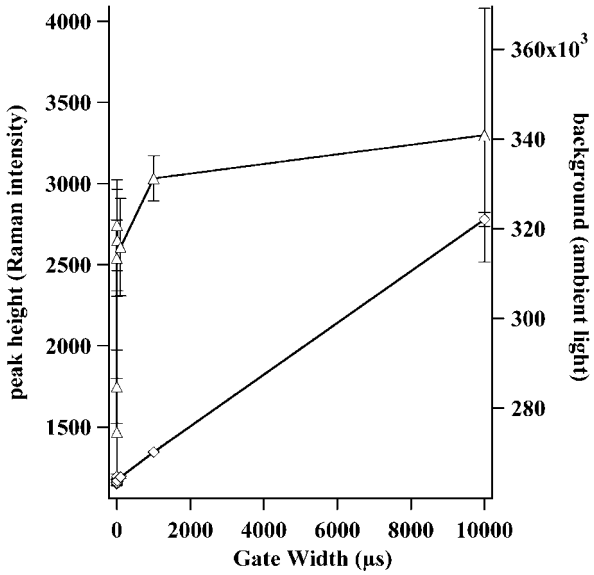

FIG. 8. A plot of the most intense peak (background subtracted) in the RDX spectrum (i.e., 880 cm^{-1}) versus detector gate width ranging from 200 ns to 10 ms. The Raman signal (open triangles, solid line) is unaffected until the gate width is decreased below ~ 1 μs. The ambient background signal (open diamonds, solid line) drops linearly as the gate width is reduced. At gate widths less than 10 ms there is virtually no background contribution to the total signal.

spectrum (i.e., 880 cm^{-1}) is shown versus detector gate width ranging from 200 ns to 10 ms. The Raman signal (open triangles, solid line) is unaffected until the gate width is decreased below ~1 μs. The ambient background signal (open diamonds, solid line) drops linearly as the gate width is reduced. At gate widths less than 10 ms there is virtually no background contribution to the total signal. Thus, the optimal gate width for this system would appear to be ~1 μs. The reason for the drop in Raman intensity beginning at 1 μs is due to electronic jitter in the timing synchronization of the pulsed laser and the ICCD. Beginning at 1 μs some of the laser pulses are out of sync with the ICCD acquisition timing and therefore are missed, reducing the Raman signal. However, the electronic jitter can easily be improved so that it is not a limiting factor. This study demonstrates the importance of characterizing the system to optimize data acquisition timing.

CONCLUSION

Recent advances in instrumentation have made it practical to develop field-portable standoff Raman systems that are suitable for identifying hazardous compounds remotely at distances up to and beyond 50 m. This work also demonstrates that standoff Raman is a viable technique for standoff measurements of HE materials. The use of a gated ICCD detector offers tremendous advantages over conventional CCDs in terms of rejecting background light and possibly long-lived luminescence and it allows measurements in ambient light conditions. However, the studies described here demonstrate that an extremely short pulse (e.g., 5 ns) laser is not required, as demonstrated for all published standoff Raman pulsed measurements, and is actually damaging to the sample. Thus, there is no need to have a laser pulse that is drastically shorter than the detector gate width. If available, a laser with a longer pulse width (<1 μs) to better match the detector gate width would be advantageous both in reducing ambient light and sample degradation. Finally, it is important to note that the 532 nm excitation wavelength used in this study was chosen based on the availability of the high throughput spectrometer and fiber-coupled probe, which already contained 532 nm laser rejection filters. This wavelength does not represent the optimal Raman excitation wavelength since many materials exhibit laser-induced fluorescence at 532 nm excitation. In fact, the use of UV laser wavelengths (e.g., below 266 nm) offers the advantages of increased Raman intensity (i.e., scales as ν^4), potential resonance Raman enhancements, a fluorescence-free window, and the ability to operate in ambient light conditions without gated detection.

ACKNOWLEDGMENTS

This work was funded in part by the Department of Defense, Grant number N00014-97-1-0806, and by the U.S. Department of Energy under grant number DOE/EPSCoR Cooperative Agreement number DE-FC02-91ER75666, amendment number A004. This work was performed under the auspices of the U.S. Department of Energy by University of California Lawrence Livermore National Laboratory under contract No. W-7405-Eng-48.

1. C. A. Heller, S. R. Greni, and E. D. Erickson, Anal. Chem. **54,** 286 (1982).
2. Y. Zhang, W. R. Seitz, and C. L. Grant, Anal. Chim. Acta **217,** 217 (1989).
3. Y. Zhang and W. R. Seitz, Anal. Chim. Acta **221,** 1 (1989).
4. C. Jian and W. R. Seitz, Anal. Chim. Acta **237,** 265 (1990).
5. R. T. Medary, Anal. Chim. Acta **258,** 341 (1992).
6. T. F. Jenkins and M. E. Walsh, Talanta **39,** 419 (1992).
7. EXPRAY and DROP-EX explosive detection kits available from Mistral Group, Web URL: http://www.mistralgroup.com/SEC_explosives.asp (accessed February 2005).
8. EDX123 explosive detection kit available from Law Enforcement Associates (LEA), Web URL: http://www.leacorp.com/product-ExplosiveDetectionKit.html (accessed April 2004).
9. L. G. Rosengren, Appl. Opt. **14,** 1960 (1975).
10. J. I. Steinfeld and J. Wormhoudt, Annu. Rev. Phys. Chem. **49,** 203 (1998).
11. K. J. Albert and D. R. Walt, Anal. Chem. **72,** 1947 (2000).
12. K. J. Albert, M. L. Myrick, S. B. Brown, D. L. James, F. P. Milanovich, and D. R. Walt, Environ. Sci. Technol. **35,** 3193 (2001).
13. A. D. Usachev, T. S. Miller, J. P. Singh, F. Y. Yueh, P. R. Jang, and D. L. Monts, Appl. Spectrosc. **55,** 125 (2001).
14. H. Sohn, M. J. Sailor, D. Magde, and W. C. Trogler, J. Am. Chem. Soc. **125,** 3821 (2003).
15. C. P. Chang, C. Y. Chao, J. H. Huang, A. K. Li, C. S. Hsu, M. S. Lin, B. R. Hsieh, and A. C. Su, Synth. Met. **144,** 297 (2004).
16. E. R. Menzel, K. K. Bouldin, and R. H. Murdock, Sci. World J. **4,** 55 (2004).
17. Committee on the Review of Existing and Potential Standoff Explosives Detection Techniques, Board on Chemical Sciences and Technology, *Existing and Potential Standoff Explosives Detection Techniques* (The National Academies Press, Washington, D.C., 2004), p. 92.
18. Y. R. Shen, *The Principles of Nonlinear Optics* (John Wiley and Sons, New York, 1991), p. 267.
19. F. W. S. Carver and T. J. Sinclair, J. Raman Spectrosc. **14,** 410 (1983).
20. C. Cheng, T. E. Kirkbridge, D. N. Batchelder, R. J. Lacey, and T. G. Sheldon, J. Forensic Sci. **40,** 31 (1995).
21. I. R. Lewis, N. W. Daniel, and P. R. Griffiths, Appl. Spectrosc. **51,** 1854 (1997).
22. N. W. Daniel, I. R. Lewis, and P. R. Griffiths, Appl. Spectrosc. **51,** 1868 (1997).
23. N. Gupta and R. Dahmani, Spectrochim. Acta, Part A **56,** 1453 (2000).
24. J. M. Sylvia, J. A. Janni, J. D. Klein, and K. M. Spencer, Anal. Chem. **72,** 5834 (2000).
25. K. Kneipp, Y. Wang, R. R. Dasari, M. S. Feld, B. D. Gilbert, J. Janni, and J. I. Steinfeld, Spectrochim. Acta, Part A **51,** 2171 (1995).
26. M. L. Lewis, I. R. Lewis, and P. R. Griffiths, Appl. Spectrosc. **58,** 420 (2004).
27. C. J. McHugh, R. Keir, D. Graham, and W. E. Smith, Chem. Commun. **6,** 580 (2002).
28. C. H. Munro, V. Pajcini, and S. A. Asher, Appl. Spectrosc. **51,** 1722 (1997).
29. L. A. Haskin, A. Wang, K. M. Rockow, B. L. Jolliff, R. L. Korotev, and K. M. Viskupic, J. Geophys. Res. **102,** 19293 (1997).
30. A. Wang, L. A. Haskin, and E. Cortez, Appl. Spectrosc. **52,** 477 (1998).
31. P. G. Lucey, T. F. Cooney, and S. K. Sharma, Lunar Planet. Sci. **29,** 1354 (1998).
32. K. A. Horton, N. Domergue-Schmidt, S. K. Sharma, P. Deb, and P. G. Lucey, Lunar Planet. Sci. **31,** 1514 (2000).
33. S. K. Sharma, S. M. Angel, M. Ghosh, H. W. Hubble, and P. G. Lucey, Appl. Spectrosc. **56,** 699 (2002).
34. T. Hirschfeld, Appl. Opt. **13,** 1435 (1974).
35. R. M. Measures, *Laser Remote Sensing, Fundamentals and Applications* (John Wiley and Sons, New York, 1984).
36. D. N. Whiteman, K. D. Evans, B. Demoz, D. O. 'C. Starr, D. Tobin, W. Feltz, G. J. Jedlovec, S. I. Gutman, G. K. Schwemmer, M. Cadirola, S. H. Melfi, and F. J. Schmidlin, J. Geophys. Res. **106,** 5211 (2000).
37. M. Wu, M. Ray, K. H. Fung, M. W. Ruckman, D. Harder, and A. J. Sedlacek III, Appl. Spectrosc. **54,** 800 (2000).
38. M. D. Ray, A. J. Sedlacek, and M. Wu, Rev. Sci. Instrum. **71,** 3485 (2000).

39. S. M. Angel, T. J. Kulp, and T. M. Vess, Appl. Spectrosc. **46,** 1085 (1992).
40. J. C. Carter, J. Scaffidi, S. Burnett, B. Vasser, S. K. Sharma, and S. M. Angel, Spectrochim. Acta, Part A, paper in press (2005).
41. H. Owen, D. E. Battey, M. J. Pelletier, and J. B. Slater, SPIE Proc. **2406,** 260 (1995).
42. K. L. McNesby, J. E. Wolfe, J. B. Morris, and R. A. Pesce-Rodriguez, J. Raman Spectrosc. **25,** 75 (1994).
43. N. F. Fell, J. M. Widder, S. V. Medlin, J. B. Morris, R. A. Pesce-Rodriguez, and K. L. McNesby, J. Raman Spectrosc. **27,** 97 (1996).
44. N. F. Fell, J. A. Vanderhoff, R. A. Pesce-Rodriguez, and K. L. McNesby, J. Raman Spectrosc. **29,** 165 (1998).
45. T. Arusi-Parpar, D. Heflinger, and R. Lavi, Appl. Opt. **40,** 6677 (2001).
46. S. K. Sharma, S. Ismail, S. M. Angel, P. G. Lucey, C. P. McKay, A. K. Misra, P. G. Mouginis-Mark, H. Newsom, U. N. Sigh, and G. J. Taylor, SPIE Proc. **5660,** paper in press (2004).